Journal of Photochemistry and Photobiology A: Chemistry 222 (2011) 77–80

Contents lists available at ScienceDirect

Journal of Photochemistry and Photobiology A: Chemistry

journal homepage: www.elsevier.com/locate/jphotochem

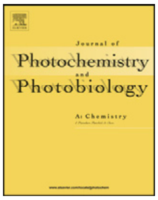

Infrared photoreaction of 2-chloroethyltrifluorosilane

Petr S. Dementyev[a,*], Anton S. Nizovtsev[a,b], Evgenii N. Chesnokov[a]

[a] Institute of Chemical Kinetics and Combustion, Institutskaya Str. 3, 630090 Novosibirsk, Russia
[b] Nikolaev Institute of Inorganic Chemistry, Lavrentiev Av. 3, 630090 Novosibirsk, Russia

ARTICLE INFO

Article history:
Received 2 April 2011
Received in revised form 9 May 2011
Accepted 21 May 2011
Available online 27 May 2011

Keywords:
2-chloroethyltrifluorosilane
Infrared photodissociation
Silicon isotopes separation

ABSTRACT

Infrared laser dissociation of 2-chloroethyltrifluorosilane has been studied in light of silicon isotopes separation. The reaction occurs via beta-elimination mechanism to yield ethylene and chlorotrifluorosilane as products. The dissociation has a relatively low energy barrier what was confirmed by high-level quantum chemical calculations. High enrichment of ^{30}Si isotope was demonstrated.

1. Introduction

Recent progress in nanofabrication makes urgent the need for isotopically pure materials [1–7]. Extremely important role of silicon for prospective quantum computing devices requires its isotopes uppermost [8–12].Silicon isotopes (*natural abundance*: ^{28}Si 92.23%, ^{29}Si 4.67%, ^{30}Si 3.10%) are currently available from the conventional gas-centrifugal separation technology [13,14]. However, the production of rare silicon isotopes ^{29}Si and ^{30}Si by this way is quite expensive [15]. Therefore many efforts have been devoted to development of alternative more economical separation methods, especially laser ones [16–21]. Molecular laser isotopes separation (*MLIS*) based on infrared multiphoton dissociation (*IR MPD*) is considered to be much attractive approach because it allows of high enrichment due to significant isotopic shifts in vibrational spectra of molecules. Although infrared laser enables to carry out a primary dissociative photoreaction with a great isotopic selectivity, secondary radical reactions essentially degrade the isotopic composition of the end products. Consequently the manufacture of rare isotopes by means of IR MPD is not so feasible.

A promising silicon MLIS scheme utilizing a photoreaction of 1,2-dichloroethyltrifluorosilane (*dCETFS*) was lately suggested in our group [22].Under infrared irradiation dCETFS undergoes the beta-elimination to form vinylchloride and chlorotrifluorosilane (CTFS). The products are stable and can be easily isolated in the individual state. The reaction has a low dissociation threshold and occurs under mild laser fluence. High isotopic selectivity over rare silicon isotopes was shown.

It is not excluded that some other organotrifluorosilanes with a halogen atom in the beta position of a side chain might behave similarly:

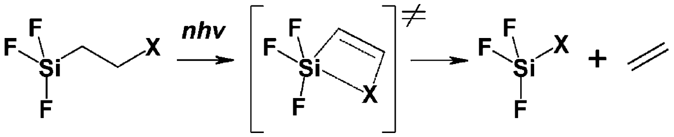

To propose the most optimal substrate for the silicon MLIS process we are continuing study of infrared photochemistry of halogenoalkyltrifluorosilanes. A potential working substrate of MLIS must satisfy certain conditions, in particular, it must be good volatile and obtainable from the main semiproducts of organosilicon industry. So the appropriate candidates for this role remain not much, namely, it could be only mono- or di-halogenated ethyltrifluorosilanes. One of them is 1,2-dibromoethyltrifluorosilane (*dBETFS*) analogous to dCETFS and being prepared from industrial reagents through two stage. But experiments revealed that photodissociation of dBETFS proceeds with a radical detachment [23].

This paper presents the experimental study of a laser photoreaction of 2-chloroethyltrifluorosilane (*CETFS*), which is derivative from one of the basic organosilicon monomers. We found that CETFS well absorbs a radiation of the carbon dioxide laser and readily undergoes a photoreaction. The reaction products were identified and a mechanism was proposed. We also measured some IR MPD parameters such as a dissociation yield and an isotopic enrichment and compared it with those of dCETFS. Potential energy profiles for CETFS and dCETFS were calculated by high-level *ab initio* methods as well.

---

[*] Corresponding author. Tel.: +7 383 333 2944; fax: +7 383 330 7350.
E-mail address: dementyev@kinetics.nsc.ru (P.S. Dementyev).

1010-6030/$ – see front matter © 2011 Elsevier B.V. All rights reserved.
doi:10.1016/j.jphotochem.2011.05.004

2. Materials and methods

2.1. Chemicals

CETFS was prepared through a fluorination of 2-chloroethyltrichlorosilane [24]. The latter was synthesized by the free-radical chlorination from commercially purchased ethyltrichlorosilane (Fluka, 97%) [25]. The final compound was purified by trap-to-trap distillation in a high-vacuum line and its purity was checked by infrared and mass spectrometry.

2.2. Experimental

Infrared photodissociation setup was previously described in detail elsewhere [21,22]. Briefly, we used a tunable pulse carbon dioxide laser for vibrational excitation and a magnetic mass-spectrometer for product analysis. The laser beam was not focused in all experiments. Infrared spectrum was obtained with a Fourier-transform spectrometer of 1 cm^{-1} in resolution.

2.3. Computational details

Geometric parameters of species under consideration were fully optimized by hybrid meta density functional M05-2X [26] with all-electron Dunning's correlation-consistent basis set of triple-zeta quality, cc-pVTZ [27], on the all atoms (next the basis set is abbreviated as VTZ). All the following single-point calculations were carried out with M05-2X/VTZ geometries. Ultrafine grid was used in all density functional theory calculations.

In order to calculate correlation of valence electrons the coupled-cluster method [CCSD(T)] [28] with VTZ basis set was applied within frozen core approximation ($E_{CCSD(T)/VTZ}$).

The correlation of the core electrons (E_{core}) was calculated at the MP2/cc-pwCVTZ level [29,30]. These effects were determined as the difference between the energy values obtained without (all-electron correlation) and with frozen core approximation.

Scalar relativistic corrections (E_{SR}) were computed as the difference between MP2(DKH)/cc-pVTZ-DK and MP2/cc-pVTZ energies [31].

Zero-point vibrational energies (E_{ZPE}) were calculated from the M05-2X/VTZ harmonic vibrational frequencies without scaling factors. The thermal correction to the enthalpy (E_{TC}) was calculated within rigid-rotor-harmonic-oscillator approximation and used for obtaining reaction enthalpies at 298 K.

Isotopic shifts for the ^{29}Si and ^{30}Si isotopomers of CETFS were also calculated at M05-2X/VTZ theoretical level.

All of the stationary points were characterized by their harmonic vibrational frequencies as minima or saddle points (number of imaginary frequencies was equal to 0 and 1 for local minima and transition states, respectively). Connections of the transition state structures between designated minima were confirmed by intrinsic reaction coordinate (IRC) calculations [32].

The calculations were performed with the use of Gaussian 03 program package [33]. Some basis sets were taken from the EMSL database [34].

Full information about results of quantum chemical calculations is placed in Supplementary material.

3. Results and discussion

3.1. Infrared spectrum and multiphoton absorption

Infrared and Raman spectra of CETFS were described earlier by Aleksa and coworkers [24]. They also showed that free CETFS molecules are the equilibrium mixture of two conformers – anti and gauche, which have slightly different vibrational frequencies. The absorption spectrum of CETFS in the region 850–1350 cm^{-1} is shown in Fig. 1A, since a working space of the carbon dioxide laser is in fact interesting for us. Very intense band (centered at 981 cm^{-1}) belonging to the Si–F stretchings is located in the laser range. We calculated that the frequency difference between conformers for these specific vibrations is small as against the bandwidth, therefore the conformers are indistinguishable for the laser. The substance can thus absorb infrared radiation, and under powerful laser field this can give a strong vibrational excitation. Furthermore, the molecules being vibrationally excited, the difference between conformers disappears at all.

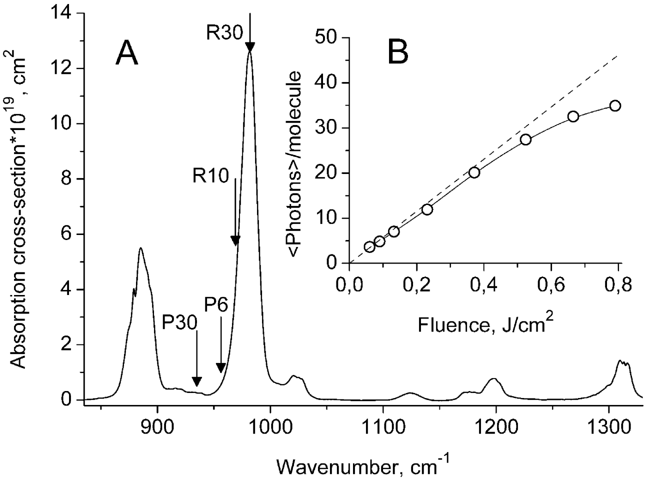

Fig. 1. (A) IR spectrum of CETFS, recorded at pressure of about 1 torr(1 torr = 133.3 Pa). Arrows show some of the CO_2 laser lines used. (B) MPA of CETFS measured at the R30 line, sample pressure was 100 mtorr. Dash line corresponds to the linear extrapolation of absorption cross-section from the IR spectrum.

We measured a multiphoton absorption (*MPA*) of CETFS, expressed as the number of quanta absorbed per a molecule depending on laser fluence (Fig. 1B). It is seen that CETFS absorbs many photons even in mild fluence conditions. This allows a rapid intramolecular heating and thus provides enough energy to overcome an activation barrier.

To anticipate a little, the infrared spectrum of CETFS is better for MLIS than that of dCETFS. Firstly, the band involved is narrower than the corresponding band of dCETFS, which is splitted. Secondly, for CETFS the band is shifted to a long-wave range as compared with dCETFS (centered at 990 cm^{-1}). So in case of CETFS the laser gap gets to the place, where the isotopic selectivity is not great, while for dCETFS the gap lies right in the spectral range of the maximum isotopic selectivity over rare isotopes.

3.2. Laser-induced reaction

CETFS readily reacts under laser action according to the equation:$F_3SiCH_2CH_2Cl \xrightarrow{nh\nu} F_3SiCl + C_2H_4$

Fig. 2 illustrates characteristic evaporation curves of a sample recorded before and after irradiation.

We cooled down a sample in a small cold finger by liquid nitrogen and then slowly heated it. Vapor pressure in a closed volume was registered as a function of evaporator temperature. This is actually the analogue of a usual distillation curve. One can see two substances are formed in equimolar quantities during reaction. And the amount equals to that of consumed CETFS. The products have quite different physical properties and thereby they can be easily separated from each other and from initial substance. In such a manner the products were simply distilled and analysed with a mass-spectrometer. These are ethylene and CTFS, it implies the

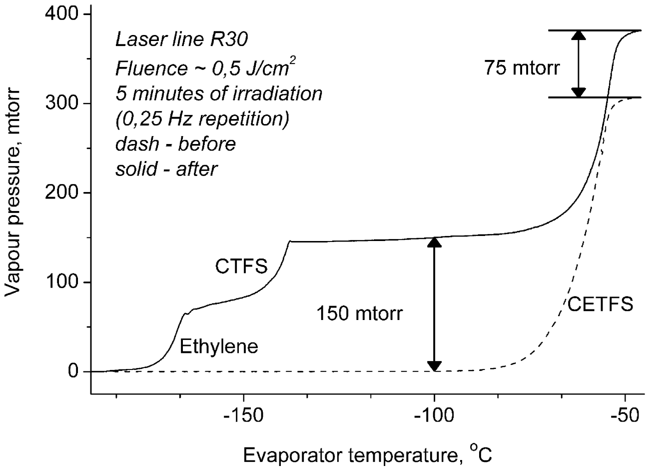

Fig. 2. Typical evaporation curves of a sample before and after reaction. The heating rate was about 0.15 K/s.

beta-elimination mechanism of reaction. Such molecular mechanism prevents the mass loss and could provide an effective MLIS process.

3.3. Dissociation yield and energy profile calculation

The reaction has a rather low activation barrier. We measured a dissociation yield as an average probability of one molecule to dissociate for a single laser pulse

$$Y = \frac{\Delta N}{N_0} \times \frac{V_{\text{irr}}}{V_0} \times \frac{1}{p}$$

where N_0 is the starting concentration, ΔN is the small concentration change during irradiation, V_{irr} is the irradiated volume of reactor, $V_0$is the full reactor volume, p is the number of introduced pulses. The dissociation yield describes indirectly a reaction rate constant in pulse experiments. In Fig. 3 the dissociation yield of CETFS depending on laser fluence is represented in comparison with the same function of dCETFS. CETFS reacts almost as easily as dCETFS. We also calculated the potential energy profiles of reaction assuming the four-membered transition states (insert in Fig. 3). The activation barriers are 45.9 and 45.3 kcal/mol for CETFS and dCETFS respectively.

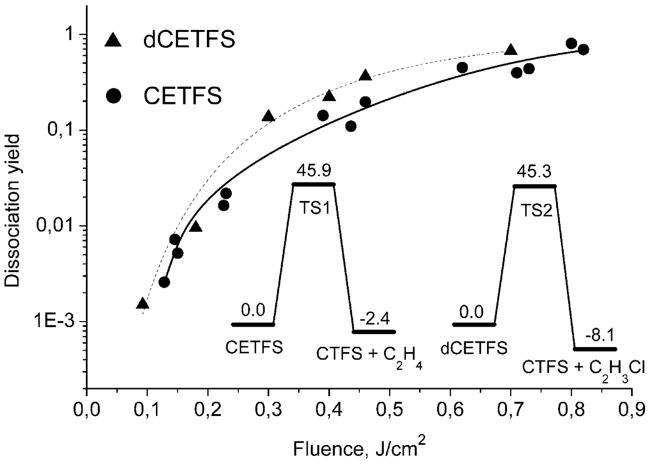

Fig. 3. Laser fluence dependence of dissociation yield of CETFS, measured at the R30 laser line. Sample pressure was 100 mtorr, relative consumption of CETFS was less 10%. The same function of dCETFS is shown for comparison (adopted from [22]). *Insert*: schematic energy profiles of reaction, calculated for CETFS and dCETFS. The scale is $\Delta(E + \text{ZPE})$ in kcal/mol.

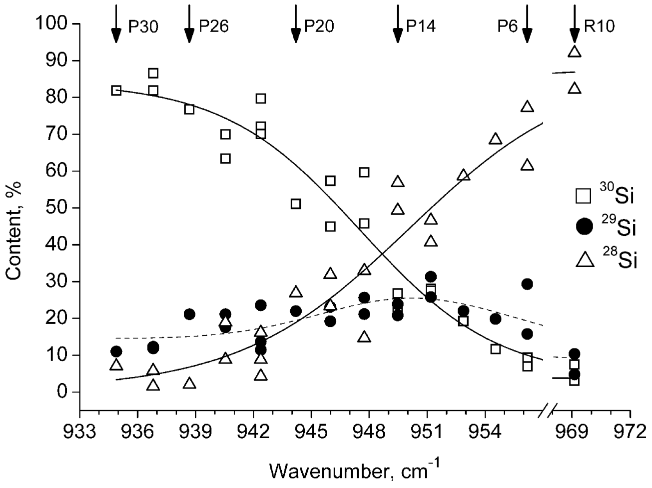

Fig. 4. Isotopic composition of product CTFS, measured mass-spectrometrically by m/z 85-87 lines of SiF_3^+ ions. CETFS pressure was 300 mtorr. Relative consumption of CETFS was kept within limits of 0.5–1.3%. Laser fluence was varied in range 0.45–0.7 J/cm^2. Arrows on the top show the location of some CO_2 laser lines used.

3.4. Isotopes separation

Very high enrichment of rare silicon isotopes was achieved in reaction product CTFS by tuning laser lines. In the Fig. 4 the silicon isotopic composition of CTFS depending on laser frequency used is shown. We accurately distilled the product and observed its mass-spectrum. Break between 957 and 968 cm^{-1} corresponds to the gap between P- and R-branches of a CO_2 laser.

The strong band at 981 cm^{-1}in the infrared spectrum of CETFS contains the spectra of three silicon isotopomers. Calculated mass-dependent red shifts for these vibrations are 7 cm^{-1} between ^{28}Si and ^{29}Si and 7 cm^{-1} between ^{29}Si and ^{30}Si isotopomers respectively. We can expect that an isotopically selective laser-induced reaction is possible.

Of course, an enrichment factor of MLIS process strongly depends on many conditions such as isotopic shifts, sample pressure and degree of conversion. In order to demonstrate the silicon isotopes separation we chose an initial sample pressure so that, on the one hand, to minimize the pressure-dependent decrease in selectivity, but on the other hand, to reliably detect the forming product. Laser energy was varied so as to make a dissociation yield moderate. When laser is tuned at the R-branch (wavenumber > 970 cm^{-1}) close to the band centre no significant isotopic enrichment is observed. In case when we move to the long-wave range of the P-branch (wavenumber < 950 cm^{-1}), the formation of ^{29}Si and ^{30}Si CTFS's isotopomers becomes preferential, and the content of ^{29}Si passes over an extremum. Near 935 cm^{-1} the content of ^{28}Si is less than 10%, but the dissociation yield becomes very low.

As mentioned above CETFS is more effective in isotopes separation than dCETFS. The maximum isotopic enrichment achieved with CETFS is 86% of ^{30}Si and 31% of ^{29}Si while in case of dCETFS the maximum contents of ^{30}Si and ^{29}Si which could be obtained are 75% and 16% respectively. We can also use a ratio of reaction rate constants (so-called isotopic selectivity) as a universal comparative feature. The maximum isotopic selectivity reached on^{30}Si is about 1650 for CETFS as against 240 for dCETFS. Regarding ^{29}Si the corresponding values are 200 for CETFS versus 35 for dCETFS.

In sum, by controlling conditions one can produce CTFS enriched by ^{30}Si up to 90% and simultaneously enhance concentration of^{28}Si in CETFS. However, the ^{29}Si isotope was found as being difficultly extracted, though the unprecedented ^{29}Si content of about 30% was achieved in our experiments. The spectral overlaps of isotopomers in initial substance seem to be too strong to permit the interjacent isotope production. In this sense CETFS does not differ from dCETFS as well as from other silicon fluorides.

4. Conclusion

CETFS readily dissociates under infrared irradiation. The reaction has a molecular mechanism, which allows of conducting an isotopically selective process. High enrichment of ^{30}Si is realizable by one stage. In whole IR MPD parameters of CETFS are better than those of dCETFS. However, if one consider the practical implementation of the silicon MLIS technology, it is necessary to determine the substance cost and its correlation to the cost of the gas-centrifugal production.

Probably, the combination of a molecular photoreaction with advanced laser schemes, such as a multi-frequency excitation, can give an excellent isotopic selectivity, even for ^{29}Si isotope.

The elimination reaction is likely to be of interest from the dynamical point of view. To clarify whether the reaction is concerted an ultrafast photodynamical study is needed.

Acknowledgments

We thank the Siberian Branch of the Russian Academy of Sciences for financial support (Grant No. 52/2009). A.S.N. is also grateful to the program of the Russian Government “Research and educational personnel of innovative Russia” (Contract No. 14.740.11.0722). The computing time on NKS-160 cluster has been provided by the Siberian Supercomputer Centre.

Appendix A. Supplementary data

Supplementary data associated with this article can be found, in the online version, at doi:10.1016/j.jphotochem.2011.05.004.

References

[1] J.W. Ager III, E.E. Haller, Phys. Status Solidi A 203 (2006) 3550.
[2] H. Watanabe, C.E. Nebel, S. Shikata, Science 324 (2009) 1425.
[3] O. Moutanabbir, D. Isheim, D.N. Seidman, Y. Kawamura, K.M. Itoh, Appl. Phys. Lett. 98 (2011) 013111.
[4] O. Moutanabbir, S. Senz, Z. Zhang, U. Gösele, Nano Today 4 (2009) 393.
[5] G. Zhang, B. Li, Nanoscale 2 (2010) 1058.
[6] C.W. Chang, A.M. Fennimore, A. Afanasiev, D. Okawa, T. Ikuno, H. Garcia, D. Li, A. Majumdar, A. Zettl, Phys. Rev. Lett. 97 (2006) 085901.
[7] N. Vandecasteele, M. Lazzeri, F. Mauri, Phys. Rev. Lett. 102 (2009) 196801.
[8] M. Kohei, Itoh, Solid State Commun. 133 (2005) 747.
[9] M.R. Rahman, M.P. Vlasenko, L.S. Vlasenko, E.E. Haller, K.M. Itoh, Solid State Commun. 150 (2010) 2275.
[10] Y. Shimizu, Y. Kawamura, M. Uematsu, M. Tomita, T. Kinno, N. Okada, M. Kato, H. Uchida, M. Takahashi, H. Ito, H. Ishikawa, Y. Ohji, H. Takamizawa, Y. Nagai, K.M. Itoh, J. Appl. Phys. 109 (2011) 036102.
[11] H. Hayashi, T. Itahashi, K.M. Itoh, L.S. Vlasenko, M.P. Vlasenko, Phys. Rev. B 80 (2009) 045201.
[12] Yasuo Shimizu, M. Kohei, K.M. Itoh, Thin Solid Films 508 (2006) 160.
[13] K.M. Itoh, J. Kato, F. Uemura, A.K. Kaliteyevskii, O.N. Godisov, G.G. Devyatych, A.D. Bulanov, A.V. Gusev, I.D. Kovalev, P.G. Sennikov, H.-J. Pohl, N.V. Abrosimov, H. Riemann, Jpn. J. Appl. Phys. 42 (2003) 6248.
[14] A.V. Gusev, A.D. Bulanov, Inorg. Mater. 44 (2008) 1395.
[15] E.E. Haller, Semiconductors 44 (2010) 841.
[16] J.L. Lyman, B.E. Newman, T. Noda, H. Suzuki, J. Phys. Chem. A 103 (1999) 4227.
[17] J. Makowe, O.V. Boyarkin, T.R. Rizzo, J. Phys. Chem. A 106 (2002) 5221.
[18] M. Polianski, O.V. Boyarkin, T.R. Rizzo, V.M. Apatin, V.B. Laptev, E.A. Ryabov, J. Phys. Chem. A 107 (2003) 8578.
[19] A. Yokoyama, H. Ohba, M. Hashimoto, K. Katsumata, H. Akagi, T. Ishii, A. Ohya, S. Arai, Appl. Phys. B 79 (2004) 883.
[20] H. Ohba, H. Akagi, K. Katsumata, M. Hashimoto, A. Yokoyama, Jpn. J. Appl. Phys. 47 (2008) 8379.
[21] P.V. Koshlyakov, S.R. Gorelik, E.N. Chesnokov, O.S. Aseev, A.A. Rakhymzhan, A.K. Petrov, Photochem. Photobiol. 85 (2009) 901.
[22] P.V. Koshlyakov, P.S. Dementyev, S.R. Gorelik, E.N. Chesnokov, A.K. Petrov, Appl. Phys. B 97 (2009) 625.
[23] P.S. Dementyev, unpublished results.
[24] V. Aleksa, A. Gruodis, P. Klaeboe, C.J. Nielsen, K. Herzog, R. Salzer, G.A. Guirgis, J.R. Durig, J. Mol. Struct. 482–483 (1999) 563.
[25] G.V. Motzarev, R.V. Dzhagazpanyan, V.R. Rosenberg, S.B. Bardenshtein, V.I. Kolbasov, T.T. Tarasova, Russ. J. Appl. Chem. 41 (1968) 2509 (in Russian).
[26] Y. Zhao, N.E. Schultz, D.G. Truhlar, J. Chem. Theory Comput. 2 (2006) 364.
[27] (a) T.H. Dunning Jr., J. Chem. Phys. 90 (1989) 1007;
(b) D.E. Woon, T.H. Dunning Jr., J. Chem. Phys. 98 (1993) 1358.
[28] (a) G.D. Purvis III, R.J. Bartlett, J. Chem. Phys. 76 (1982) 1910;
(b) K. Raghavachari, G.W. Trucks, J.A. Pople, M. Head-Gordon, Chem. Phys. Lett. 157 (1989) 479.
[29] C. Møller, M.S. Plesset, Phys. Rev. 46 (1934) 618.
[30] K.A. Peterson, T.H. Dunning Jr., J. Chem. Phys. 117 (2002) 10548.
[31] (a) M. Douglas, N.M. Kroll, Ann. Phys. (NY) 82 (1974) 89;
(b) B.A. Hess, Phys. Rev. A32 (1985) 756;
(c) B.A. Hess, Phys. Rev. A33 (1986) 3742;
(d) W.A. de Jong, R.J. Harrison, D.A. Dixon, J. Chem. Phys. 114 (2001) 48.
[32] (a) K. Ishida, K. Morokuma, A. Kormornicki, J. Chem. Phys. 66 (1977) 2153;
(b) C. Gonzalez, H.B. Schlegel, J. Chem. Phys. 90 (1989) 2154;
(c) C. Gonzalez, H.B. Schlegel, J. Phys. Chem. 94 (1990) 5523.
[33] M.J. Frisch, G.W. Trucks, H.B. Schlegel, G.E. Scuseria, M.A. Robb, J.R. Cheeseman, J.A. Montgomery Jr, T. Vreven, K.N. Kudin, J.C. Burant, J.M. Millam, S.S. Iyengar, J. Tomasi, V. Barone, B. Mennucci, M. Cossi, G. Scalmani, N. Rega, G.A. Petersson, H. Nakatsuji, M. Hada, M. Ehara, K. Toyota, R. Fukuda, J. Hasegawa, M. Ishida, T. Nakajima, Y. Honda, O. Kitao, H. Nakai, M. Klene, X. Li, J.E. Knox, H.P. Hratchian, J.B. Cross, V. Bakken, C. Adamo, J. Jaramillo, R. Gomperts, R.E. Stratmann, O. Yazyev, A.J. Austin, R. Cammi, C. Pomelli, J.W. Ochterski, P.Y. Ayala, K. Morokuma, G.A. Voth, P. Salvador, J.J. Dannenberg, V.G. Zakrzewski, S. Dapprich, A.D. Daniels, M.C. Strain, O. Farkas, D.K. Malick, A.D. Rabuck, K. Raghavachari, J.B. Foresman, J.V. Ortiz, Q. Cui, A.G. Baboul, S. Clifford, J. Cioslowski, B.B. Stefanov, G. Liu, A. Liashenko, P. Piskorz, I. Komaromi, R.L. Martin, D.J. Fox, T. Keith, M.A. Al-Laham, C.Y. Peng, A. Nanayakkara, M. Challacombe, P.M.W. Gill, B. Johnson, W. Chen, M.W. Wong, C. Gonzalez, J.A. Pople, Gaussian 03, Revision E.01, Gaussian, Inc., Wallingford CT, 2004.
[34] EMSL basis set library. http://www.emsl.pnl.gov/forms/basisform.html.